Tumor-Localized Ligation of CD3 and CD28 with Systemic Regulatory T-Cell Depletion Induces Potent Innate and Adaptive Antitumor Responses

Chien-Hsin Lee,[1] Yi-Hsuan Chiang,[2] Shih-En Chang,[2] Chin-Liew Chong,[2] Bing-Mae Cheng,[2] and Steve R. Roffler[2]

Abstract

Purpose: Tumor-localized activation of immune cells by membrane-tethered anti-CD3 antibodies (CD3L) is under investigation to treat poorly immunogenic tumors. Here we sought to elucidate the mechanism of antitumor immunity elicited by CD3L.

Experimental Design: CD3L and CD86 were expressed on poorly immunogenic B16 melanoma cells (B16/3L86 cells) and the effect of various lymphocytes, including $CD4^+$ and $CD8^+$ T cells, natural killer T (NKT) cells, and regulatory T cells, on antitumor activity was investigated.

Results: B16/3L86 cells activated naïve T cells; suppressed tumor growth in subcutaneous, peritoneal, and metastasis models; and protected mice from rechallenge with B16 melanoma cells. However, *in vivo* antitumor activity against primary B16/3L86 tumors unexpectedly depended on NKT cells rather than $CD4^+$ or $CD8^+$ T cells. Treatment of mice with low-dose cyclophosphamide or anti-CD25 antibody to deplete regulatory T cells unmasked latent T-cell antitumor activity; the number of activated $CD8^+$ T cells in tumors increased and B16/3L86 tumors were completely rejected in a $CD8^+$ and $CD4^+$ T-cell – dependent fashion. Furthermore, fibroblasts expressing CD3L and CD86 suppressed the growth of neighboring B16 cancer cells *in vivo*, and direct intratumoral injection of adenoviral vectors expressing CD3L and CD86 or CD3L and a membrane-tethered anti-CD28 antibody significantly suppressed the growth of subcutaneous tumors.

Conclusions: Tumor-located ligation of CD3 and CD28 can activate both innate (NKT cells) and adaptive ($CD4^+$ and $CD8^+$ T cells) responses to create a tumor-destructive environment to control tumor growth, but modulation of regulatory T cells is necessary to unmask local adaptive antitumor responses.

Anti-CD3 antibody – based therapies have been widely investigated for the treatment of cancer. Systemic administration of anti-CD3 antibodies was found to produce antitumor activity in patients but polyclonal activation of T cells caused severe side effects due to widespread release of cytokines (1, 2). More localized activation of T cells in tumors can be achieved by using bispecific antibodies in which an anti-CD3 antibody is linked or fused to an antibody against antigens expressed on cancer cells. Bispecific antibodies have shown good antitumor activity both in animal models (3) and in clinical trials (4, 5). However, limited cytolytic activity, low potency, and side effects associated with systemic T-cell activation have hampered more widespread utilization of bispecific antibodies (6). More recently, novel potent bispecific antibody constructs are showing impressive anticancer activity in clinical trials (7), emphasizing the potential of tumor-located ligation of CD3 on tumor-infiltrating lymphocytes (TIL) for improved cancer management.

Activation of lymphocytes by membrane-tethered immune-stimulatory antibodies expressed locally on cancer cells provides an alternative treatment that retains benefits of bispecific antibodies while minimizing the adverse effects associated with systemic antibody administration. In this strategy, antibodies with specificity for activation receptors present on lymphocytes are expressed on the surface of cancer cells by fusing the antibody to a transmembrane domain or glycosylphosphatidylinositol anchor (8). We and others have shown that membrane-tethered antibodies with specificity for CD3 or the T-cell receptor can potently trigger activation of naïve T cells and significantly suppress tumor growth in mice (9 – 12). Likewise, tumor-located expression of a membrane-tethered antibody against CD137, which is expressed on T cells, monocytes, dendritic cells, and natural killer (NK) cells, caused

Authors' Affiliations: [1]Molecular Medicine Program, Taiwan International Graduate Program, Institute of Biomedical Sciences, and [2]Institute of Biomedical Sciences, Academia Sinica, Taipei, Taiwan

Received 9/5/08; revised 12/9/08; accepted 12/9/08; published OnlineFirst 3/24/09.

Grant support: Academia Sinica grant AS91IBMS3PP and National Science Council grant NSC96-2628-B001-003-MY3 (S.R. Roffler).

The costs of publication of this article were defrayed in part by the payment of page charges. This article must therefore be hereby marked *advertisement* in accordance with 18 U.S.C. Section 1734 solely to indicate this fact.

Note: Supplementary data for this article are available at Clinical Cancer Research Online (http://clincancerres.aacrjournals.org/).

Requests for reprints: Steve Roffler, Room N232, Institute of Biomedical Sciences, Academia Sinica, Academia Road, Section 2, No. 128, Taipei 11529, Taiwan. Phone: 886-2-2652-3079; Fax: 886-2-2782-9142; E-mail: sroff@ibms.sinica.edu.tw.

doi:10.1158/1078-0432.CCR-08-2311

Translational Relevance

Cancer immunotherapy is difficult because most tumors are poorly immunogenic. Activation of lymphocytes by membrane-tethered immune-stimulatory antibodies is under investigation to treat poorly immunogenic tumors. We found that expression of anti-CD3 scFv and CD86 on poorly immunogenic cancer cells produced strong natural killer T-cell antitumor activity in the presence of regulatory T cells, whereas both natural killer T cells and $CD8^+$ T cells provided strong antitumor activity after regulatory T cells were depleted from mice. Expression of anti-CD3 scFv and CD86 on cells induced bystander cytotoxicity to neighboring cancer cells in tumors. Direct injection of recombinant adenoviral vectors expressing CD3L and CD86 also produced antitumor activity in subcutaneous tumors. Thus, local expression of membrane-tethered CD3 antibody and CD86 can create a tumor destruction environment that may lead to clinical approaches for cancer therapy. Our results also have important implications for enhancing the efficacy of anti-CD3 bispecific antibody cancer treatment.

extensive rejection of poorly immunogenic tumors in mice (13, 14). Similarly, tumor cells engineered to express membrane-tethered anti-CD16 scFv induced NK cell cytotoxicity and phagocytosis of tumor cells by macrophages in mice (15). Local expression of immune-stimulatory antibodies may facilitate more selective activation of TILs and minimize systemic activation of immune cells, which can lead to unwanted toxicity.

Tumor-infiltrating regulatory T cells (Treg) play a crucial role in tumor immune evasion and are an obstacle for successful tumor therapy (16). Due to their immunoregulatory function, Tregs can induce antigen-specific and nonspecific inhibition of T-cell activity (17, 18). Clinically, Tregs have been found to accumulate in tumors of patients with ovarian cancer, lung cancer, melanoma, pancreatic cancer, breast cancer, and cervical cancer (19–23). Agents that deplete or inhibit Treg function can reverse suppression and promote T-cell–mediated cytotoxicity (24–26). However, it is currently unknown how Tregs affect the antitumor activity of lymphocytes that are directly activated in tumors by membrane-tethered antibodies.

NK cells are a subset of lymphocytes that express CD16 and a variety of activating and inhibiting receptors on their surface (27). A major role of NK cells is surveillance of cells, such as those infected with viruses, which display low levels of MHC class I molecules. NKT cells are a T-cell subset defined by the coexpression of a T-cell receptor and NK-cell markers. Most NKT cells express an invariant T-cell receptor α chain with reactivity for the glycosphingolipid α-galactosylceramide presented by the class I–like molecule CD1d (28). A distinguishing feature of NKT cells is their rapid production of multiple cytokines within hours of their activation.

The goal of this study was to elucidate the mechanism of the antitumor immune responses generated by tumor-located expression of membrane-tethered anti-CD3 antibodies. We hypothesized that direct activation of TILs might produce strong antitumor activity to overcome low tumor immunogenicity and Treg-mediated suppression of tumor immune responses. To test this, we examined the immune response against B16 melanoma cells that were engineered to express a membrane-tethered anti-CD3 antibody as well as CD86 to provide costimulation to T cells (10). B16 melanoma cells were studied because these poorly immunogenic tumors are infiltrated with Tregs (29). We show that expression of membrane-tethered anti-CD3 antibodies on B16 cells induced strong NKT antitumor activity and T-cell–mediated protection against subsequent challenge with unmodified B16 cancer cells, whereas direct T-cell antitumor activity was greatly enhanced by systemic Treg depletion.

Materials and Methods

Mice and cell lines. Female C57BL/6, BALB/c, and CD8-deficient ($CD8a^{-/-}$, C57BL/6 background) mice were maintained in the Animal Center in the Institute of Biomedical Sciences (Taipei, Taiwan) under specific pathogen-free conditions. CD1d-deficient ($CD1d^{-/-}$) mice were kindly provided by Dr. C. Wang (University of Chicago, Chicago, IL). Beige/severe combined immunodeficient mice were from the National Taiwan University (Taipei, Taiwan). All experiments were conducted in accordance with institutional guidelines for animal care and use.

B16F1 melanoma cells (B16 cells) were acquired from American Type Culture Collection. B16/3L, B16/Ox, B16/3L86, and B16/Ox86 cells denote B16 cells that expressed CD3L (membrane-tethered anti-CD3 scFv), membrane-anchored anti-phOx scFv (control scFv), CD3L and CD86, or anti-phOx scFv and CD86, respectively (9). To generate B16/3L and B16/Ox cells, B16 cells were transfected with pLNCX-based vectors (Clontech) encoding anti-CD3 or anti-phOx scFv and selected in medium containing 1.2 mg/mL G418. B16/3L86 and B16/Ox86 cells were generated by cotransfecting B16 cells with pcDNA3.1/zeo–based vectors (Invitrogen) encoding murine CD86 and pLNCX-based vectors encoding anti-CD3 or anti-phOx scFv genes and selecting in medium containing 1.2 mg/mL G418 and 0.4 mg/mL zeocin. BALB/c 3T3 fibroblasts were obtained from National Health Research Institutes (Hsin Chu, Taiwan). 3T3/3L86 cells were generated by transfecting 3T3 cells with vectors encoding CD3L and CD86 and selecting in medium containing 1.2 mg/mL G418 and 0.4 mg/mL zeocin. TSA murine breast adenocarcinoma cells were kindly provided by Dr. P. Lollini (University of Bologna, Bologna, Italy). Cells were cultured in DMEM supplemented with 10% bovine serum and 1.2 mg/mL G418 alone or with 0.4 mg/mL zeocin at 37°C in an atmosphere of 5% CO_2.

In vivo *tumor growth.* Groups of five to seven C57BL/6 mice were s.c. injected with 2×10^6 wild-type (wt) or transfected B16 cells on their left flank (unless otherwise specified). Tumor dimensions were estimated as 0.5 × height × width × length. Mice were sacrificed when tumor size exceeded 2,000 mm^3. Mice that did not develop tumors within 60 d of initial tumor inoculation were rechallenged with 1×10^5 B16 cells. For the experimental lung metastasis model, 10^5 wt or transfected B16 cells were i.v. injected via the tail vein of C57BL/6 mice. Mice were sacrificed 20 d after tumor inoculation to count lung tumor colonies under a dissecting microscope. Wt or transfected B16 tumor cells (10^6) were i.p. injected in groups of C57BL/6 mice to establish an i.p. tumor model. Mice that showed signs of illness or fatigue were killed. For assessing bystander killing effects, 2×10^6 B16 melanoma cells were mixed with B16/3L86 tumor cells or 3T3/3L86 cells at a ratio of 1:1 and then injected s.c. into C57BL/6 mice. Likewise, 5×10^5 TSA adenocarcinoma cells were mixed with an equal number of 3T3/3L86 cells before s.c. injection in BALB/c mice. Tumor growth was monitored for 60 d.

T-cell enrichment. Splenocytes isolated from C57BL/6 mice were treated with ACK buffer (0.15 mol/L NH_4Cl, 10 mmol/L $KHCO_3$, 0.1 mmol/L Na_2EDTA, pH 7.2) to lyse RBC and then allowed to attach to culture plates for 2 h. Cells remaining in suspension were transferred to

culture plates coated with 100 μg of goat anti-mouse IgM, IgG, and IgA antibodies for 45 min at 37°C. Nonadherent cells were labeled with CD8a (Ly-2) microbeads and collected in an MS cell separation column according to the manufacturer's instructions (Miltenyi Biotech). Unbound cells were labeled with CD4 (L3T4) microbeads and purified in a similar fashion. The purity of enriched $CD8^+$ and $CD4^+$ T cells was 90% to 98% as determined by fluorescence-activated cell sorting (FACS).

Isolation of peritoneal mononuclear cells. Peritoneal exudate cells were retrieved by peritoneal lavage with 7 mL of DMEM supplemented with 10% bovine serum per mouse. The exudate cells were centrifuged and resuspended in 3 mL DMEM supplemented with 10% bovine serum. The cell suspension was then layered on top of 3 mL of Ficoll-Histopaque 1083 (Sigma-Aldrich) and centrifuged at 400 × *g* for 30 min. The opaque layer at the interface was recovered in PBS for further experiments.

Cytotoxicity assay. B16 or B16/3L86 tumor cells (10^6) were labeled with 0.5 μCi [^{3}H]thymidine in six-well plates for 16 h at 37°C. Naïve $CD8^+$ and $CD4^+$ cells were incubated with the [^{3}H]thymidine-labeled cells (1×10^4 cells per well in 96-well round-bottomed plates) in triplicate at graded ratios for 72 h at 37°C. Nonadherent cells were then removed by repeatedly washing the wells. The radioactivity of adherent cells was measured in a TopCount Microplate Scintillation Counter (Packard). The percentage of specific lysis was calculated as follows: % specific lysis = [(spontaneous cpm - experimental cpm) / spontaneous cpm] × 100%.

Effect of IFN-γ on cell growth. B16 or B16 transfectant cells (10,000) in triplicate 96-well microtiter wells were incubated with defined amounts of murine IFN-γ for 24 h. The cells were then pulsed with 1 μCi [^{3}H]thymidine for an additional 24 h. The radioactivity of the cells was measured in a TopCount Microplate Scintillation Counter as described above.

T-cell proliferation. Tumor cells were suspended in PBS and treated with 100 μg/mL mitomycin C for 2 h at 37°C. The cells were then washed thrice and incubated with enriched $CD4^+$ and $CD8^+$ cells at a ratio of 1:10 (antigen-presenting cells/T cells) in triplicate in round-bottomed 96-well plates for 48 h before adding 1 μCi of [^{3}H]thymidine per well for another 16 h. The cells were harvested and the radioactivity was measured with a TopCount Microplate Scintillation Counter (Packard).

FACS analysis and antibodies. Cells were blocked in FACS staining buffer (PBS containing 0.1% bovine serum albumin and 0.01% sodium azide) for 40 min at 4°C with 2 μg/mL anti-FcγRII/III antibody (clone

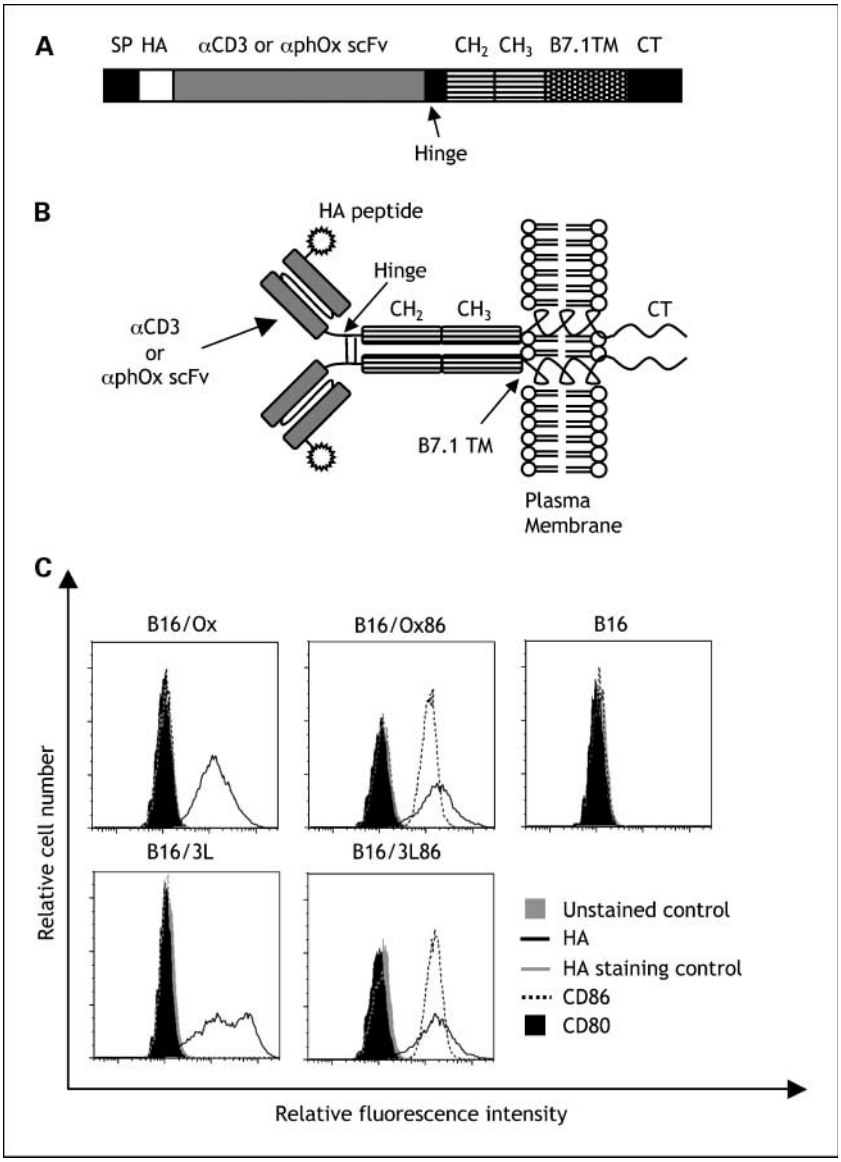

Fig. 1. Expression of CD3L and CD86 on B16 melanoma cells. *A,* illustration of membrane-tethered antibody gene construct. This construct codes for a signal peptide (*SP*), a HA epitope (*HA*), a scFv, the hinge, CH_2 and CH_3 domains of the human IgG1 heavy chain, and the murine B7.1 transmembrane (*TM*) domain and cytoplasmic tail (*CT*). *B,* the predicted structure of CD3L or Ox. Chimeric scFv can form disulfide-linked dimers on the cell surface. *C,* B16 cells and stable B16 transfectants were immunofluorescence stained for membrane-tethered anti-CD3 scFv (CD3L) or anti-phOx scFv (Ox; HA epitope, *solid lines*) as well as for CD86 (*dotted lines*) and CD80 (*solid black curves*). Results show the immunofluorescence of 10,000 cells measured by FACS.

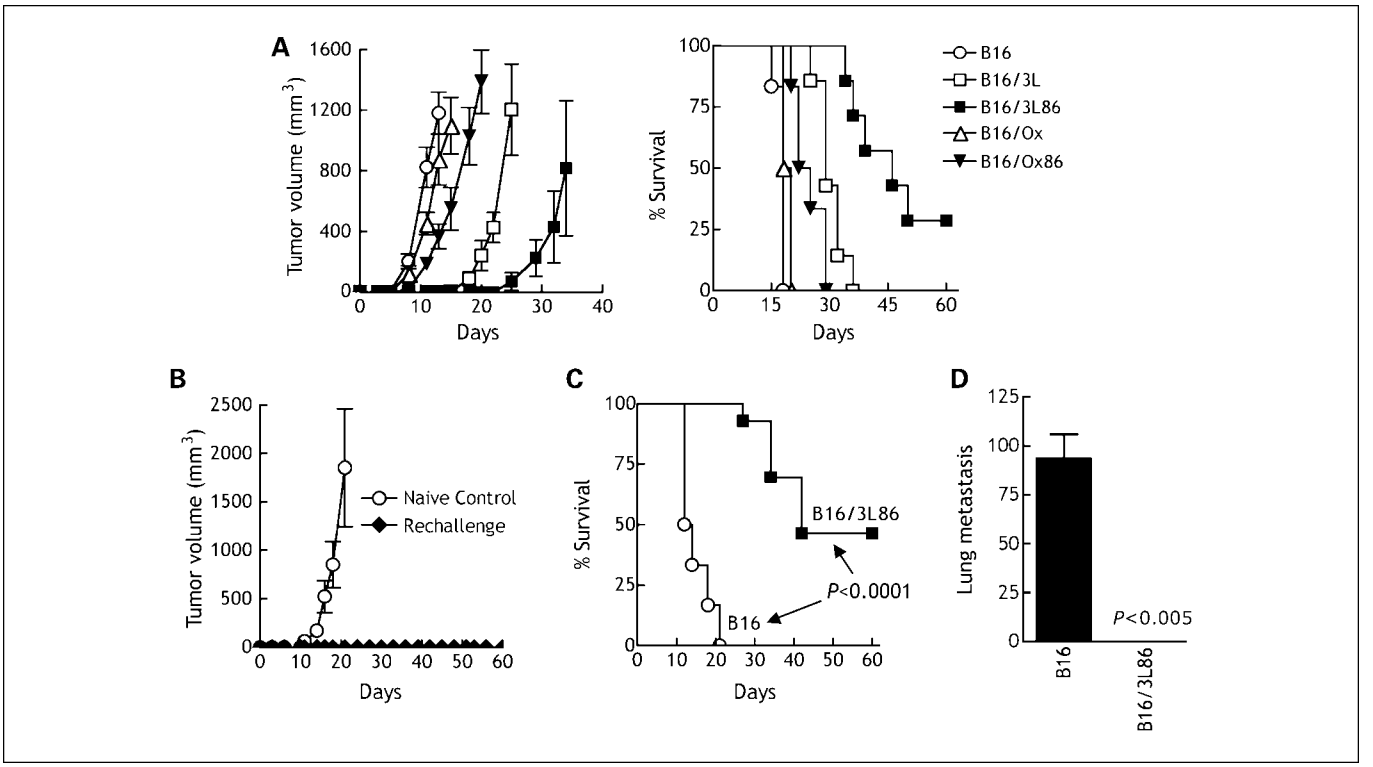

Fig. 2. Expression of CD3L and CD86 on B16 melanoma cells suppresses tumor growth in immunocompetent mice. *A,* groups of six to seven C57BL/6 mice were s.c. injected with 2×10^6 B16 cells or B16 transfectants and tumor growth (*left*) and survival (*right*) were monitored. This experiment was repeated thrice with similar results. Bars, SE. *B,* six mice remaining tumor-free for at least 60 d after s.c. inoculation with B16/3L86 cells from three independent experiments as described in *A* were challenged with 1×10^5 B16 cells. Five age-matched naïve mice were also injected as a control. *C,* C57BL/6 mice ($n = 6$) were i.p. injected with 10^6 B16 or B16/3L86 cells and mouse survival was monitored. *D,* C57BL/6 mice ($n = 6$) were i.v. inoculated with 2×10^5 B16 or B16/3L86 cells. Mice were killed on day 21 and tumor colonies in their lungs were enumerated under a dissecting microscope. This experiment was repeated once with similar results. Bars, SE.

2.4G2, BD Pharmingen), then labeled for 40 min with the appropriate specific antibodies followed by staining with propidium iodine at 5 μg/mL. For intracellular staining of FoxP3 and IFN-γ, cells were fixed with 4% paraformaldehyde and permeabilized with 0.1% saponin and 5% bovine serum albumin in PBS. The following antibodies were used: biotin-rat anti-mouse CD86 (clone GL1), biotin-hamster anti-mouse CD80 (clone 16-10A1), FITC-hamster anti-mouse CD3ε (clone 145-2C11), phycoerythrin (PE)-rat anti-mouse CD4 (clone L3T4), PE-rat anti-mouse CD8 (clone Ly-2), PE-mouse anti-mouse NK1.1 (clone PK136), PE-rat IgG1 (clone R3-34), allophycocyanin-hamster anti-mouse CD3ε (clone 145-2C11, all BD Pharmingen), Alexa Fluor 488-rat anti-mouse CD8 (clone 53-6.7, Biolegend), PE-rat anti-mouse IFN-γ (clone XMG1.2, Biolegend), rat anti-hemagglutinin (HA; clone 3F10, Roche), FITC-goat anti-rat IgG(H+L) (Jackson ImmuoResearch), PE-rat anti-mouse Rae-1 (clone 186107, R&D Systems), rat anti-mouse MULT-1 (clone 237104, R&D Systems), PE-rat anti-mouse H60 (clone 205326, R&D Systems), FITC-rat anti-mouse CD1d (clone 1B1, eBioscience), and Alexa Fluor 647-rat anti-mouse/rat FoxP3 (clone FJK/-16S, eBioscience). The stained cells were then analyzed on a FACSCanto using FACSDiva software (both BD Biosciences). Only viable cells, determined on the basis of their forward scatter/side scatter and propidium iodine staining (propidium iodine – positive cells were excluded), were used in the analyses.

In vivo *depletion of CD4$^+$, CD8$^+$, and NK1.1$^+$ cells.* On days -8, -7, and -6, groups of mice received i.p. injections of 0.5 mg anti-CD4 (clone GK1.5, American Type Culture Collection), anti-CD8 (clone 53-6.7, American Type Culture Collection), or control antibody (HAA.1E8, kindly provided by Dr. M. H. Tao, Institute of Biomedical Sciences, Academia Sinica, Taipei, Taiwan) before s.c. tumor inoculation. Mice then received i.p. injections of 0.25 mg of the corresponding antibodies every 3 d. For depletion of NK1.1$^+$ cells, mice were i.p. injected with 0.5 mg of anti-NK1.1 (clone PK136, American Type Culture Collection) antibody every 7 d starting 7 d before tumor inoculation. Peripheral blood mononuclear cells of mice were analyzed by FACS to verify specific depletion.

Adenovirus-mediated therapy. pJM17 harboring the adenovirus genome and pAd-cytomegalovirus shuttle vector were kindly provided by Dr. S.K. Shyue (Institute of Biomedical Sciences, Academia Sinica, Taipei, Taiwan). cDNAs for membrane-tethered scFv and CD86 were cloned into pAd-cytomegalovirus and then cotransfected with pJM17 in 293N cells to produce recombinant adenovirus expressing CD3L (Ad/3L), CD86 (Ad/86), anti-phOx scFv (Ad/Ox), or anti-CD28 scFv (Ad/28L). BALB/c mice were s.c. inoculated with 5×10^5 TSA tumor cells on day 0. On days 11 and 12, 10^9 plaque-forming units of Ad/3L were mixed with or without 10^9 plaque-forming units of Ad/86 or Ad/28L and directly injected into established TSA tumors in mice. As control groups, 10^9 plaque-forming units of Ad/Ox were also mixed with 10^9 plaque-forming units of Ad/86 or Ad/28L before intratumoral injection. Tumor growth was followed for 60 d.

Statistics. Data of s.c. tumor growth, T-cell – mediated cytotoxicity, and lung metastasis were analyzed using two-way ANOVA. T-cell proliferation and peritoneal cell phenotyping were analyzed by two-sided Student's *t* test. Animal survival was analyzed by the two-sided log-rank test. All analyses were done with GraphPad Prism 4 software. $P \leq 0.05$ was considered statistically significant.

Results

In vivo *antitumor activity of membrane-tethered CD3L and CD86.* Transgenes encoding membrane-anchored anti-CD3

scFv (CD3L) or anti-phOx scFv (Ox; Fig. 1A and B) were transfected individually or with the CD86 costimulatory molecule to obtain stable B16 melanoma cell lines expressing CD3L (B16/3L), Ox (B16/Ox), or these membrane-tethered antibodies along with CD86 (B16/3L86 and B16/Ox86, respectively; Fig. 1C). The phOx scFv specifically recognizes the chemical hapten 4-ethoxy-methylene-2-phenyl-2-oxazolin-5-one (30). This scFv does not bind lymphocytes and was used as a negative control membrane-anchored antibody. Figure 1C also shows that none of the cells expressed endogenous CD80 and only those cells transfected with the CD86 expression vector (B16/3L86 and B16/Ox86) expressed CD86. The *in vitro* growth rates of B16, B16/3L, and B16/Ox cells were similar with doubling times of 14 to 15 hours (Supplementary Fig. S1). B16/3L86 and B16/Ox86 cells grew slightly slower with doubling times of 16.5 and 18 hours, respectively, possibly due to the need to culture the cells in both G418 and zeocin. In agreement with our previous results (9), subcutaneous B16/3L tumor growth was delayed as compared with B16 tumors in C57BL/6 mice (Fig. 2A; Table 1), indicating that ligation of CD3 can induce lymphocyte antitumor activity. Coexpression of CD3L and CD86 on B16 cells (B16/3L86 cells) greatly enhanced tumor suppression and significantly enhanced the survival of tumor challenged mice, with two of six mice remaining tumor-free through 60 days of observation (Fig. 2A). Suppression of tumor growth depended on ligation of CD3 because B16 cells expressing the membrane-tethered control antibody (B16/Ox and B16/Ox86) formed tumors that progressed rapidly in C57BL/6 mice at rates that were similar to B16 tumors. Importantly, mice that rejected B16/3L86 tumors developed systemic antitumor memory as shown by protection of 100% of mice from a subsequent challenge with unmodified B16 tumor cells (Fig. 2B). Expression of CD3L and CD86 on B16 cells also remarkably extended the life span of i.p. tumor-grafted mice (Fig. 2C). The peritoneum of B16 cell–injected mice was filled with large clusters of tumors, whereas only a few small tumor nodules (<0.2 mm in diameter) were observed in the peritoneum 8 days after inoculation of B16/3L86 cells (data not shown). Expression of CD3L and CD86 on B16 cells also completely suppressed the formation of lung tumor colonies in an experimental metastasis model (Fig. 2D). These results clearly show that membrane-tethered CD3L and CD86 can strongly suppress the growth of poorly immunogenic B16 melanomas in subcutaneous, peritoneal, and metastatic tumor models.

CD4$^+$ and CD8$^+$ T cells are not required for the rejection of B16/3L86 tumors. B16/3L cells triggered modest *in vitro* proliferation of naïve CD4$^+$ and CD8$^+$ T cells, but as expected, coexpression of CD86 with CD3L on B16 cells greatly enhanced T-cell proliferation (B16/3L86 cells in Fig. 3A). To determine if expression of CD3L and CD86 on B16 cells could induce CTL activity to these poorly immunogenic melanoma cells, naïve CD4$^+$ and CD8$^+$ T cells were cultured with B16 or B16/3L86 cells at defined ratios for 3 days. B16/3L86 cells, but not B16 cells, induced strong CD8$^+$ T-cell–mediated cytotoxicity (Fig. 3B). By contrast, no significant killing was observed when CD4$^+$ T cells were incubated with either B16 or B16/3L86 cells (Fig. 3B).

The fact that naïve CD8$^+$ T cells can be directly induced to kill B16/3L86 tumor cells suggested that CD8$^+$ T cells may play an important role in mediating *in vivo* antitumor activity against B16/3L86 tumors. However, repression of B16/3L86 tumors was equally effective in C57BL/6 mice or in transgenic mice lacking CD8$^+$ T cells (Fig. 3C). Likewise, depletion of CD4$^+$ T cells in CD8$^{-/-}$ mice did not hinder suppression of B16/3L86 tumor growth, indicating that neither CD8$^+$ nor CD4$^+$ T cells were necessary for control of B16/3L86 tumor growth (Fig. 3C). To verify these results, we used specific antibodies to deplete CD4$^+$ and CD8$^+$ T cells in C57BL6 mice. In agreement with the results in CD8$^{-/-}$ mice, B16/3L86 tumor growth was still suppressed after antibody-mediated depletion of CD4$^+$ or CD8$^+$ T cells (Fig. 3D). These results clearly show that CD8$^+$ and CD4$^+$ T cells are dispensable for primary rejection of B16/3L86 tumors.

Role of NKT cells in suppression of B16/3L86 tumors. Besides conventional T cells, NKT cells also express CD3 (31). To investigate if NKT cells play a role in the antitumor activity displayed by CD3L, groups of C57BL/6 mice were injected with an antibody against NK1.1 before s.c. injection of B16 or B16/3L86 melanoma cells. This antibody can deplete NKT and NK cells (32). All mice depleted of NK1.1$^+$ cells developed B16/3L86 tumors and displayed significantly reduced survival times as compared with mice treated with a control antibody (Fig. 4A). Because the NK1.1 marker is expressed on both NK and NKT cells and antibody depletion of immune cells may be incomplete, we also inoculated CD1d$^{-/-}$ mice, which lack classic NKT cells, with B16 or B16/3L86 cells. The survival times of C57BL/6 and CD1d$^{-/-}$ mice bearing B16 tumors were similar, whereas the survival of CD1d$^{-/-}$ mice bearing B16/3L86 tumors was significantly reduced as compared with C57BL/6 mice (Fig. 4B). These results show a critical role for NKT cells in controlling the growth of B16/3L86 tumors. None of the B16 transfectants expressed the class I–like molecule CD1d, which can present glycosphingolipids to NKT cells (Supplementary Fig. S2). The B16 transfectants also did not express the NKG2D ligand H60, MULT-1, or Rae-1 (Supplementary Fig. S2), consistent with NKT cell activation by CD3L and CD86 on the B16/3L86 cells. IFN-γ is a key mediator of NKT cells (33). Consistent with a role of NKT cells in controlling tumor growth, B16/3L86 cells rapidly progressed in IFN-γ–deficient mice, showing that IFN-γ was indispensable for suppression of B16/3L86 tumors (Fig. 4C). In agreement with a previous report (34), B16 cells and transfectants were directly sensitive to IFN-γ *in vitro*, resulting in profound growth delay (Supplementary Fig. S3). All the cells displayed similar sensitivity to IFN-γ.

Depletion of Tregs improves tumor suppression by unmasking the antitumor activity of CD8$^+$ T cells. B16/3L86 tumor cells effectively activated CD8$^+$ T cells *in vitro* (Fig. 3A and B) and

Table 1. Significant difference between B16/3L86 and other groups

	P value vs B16/3L86	
	Tumor growth	**Survival**
B16	<0.0001	<0.001
B16/3L	<0.0001	<0.005
B16/3L86	—	—
B16/Ox	<0.0001	<0.001
B16/Ox86	<0.0001	<0.01

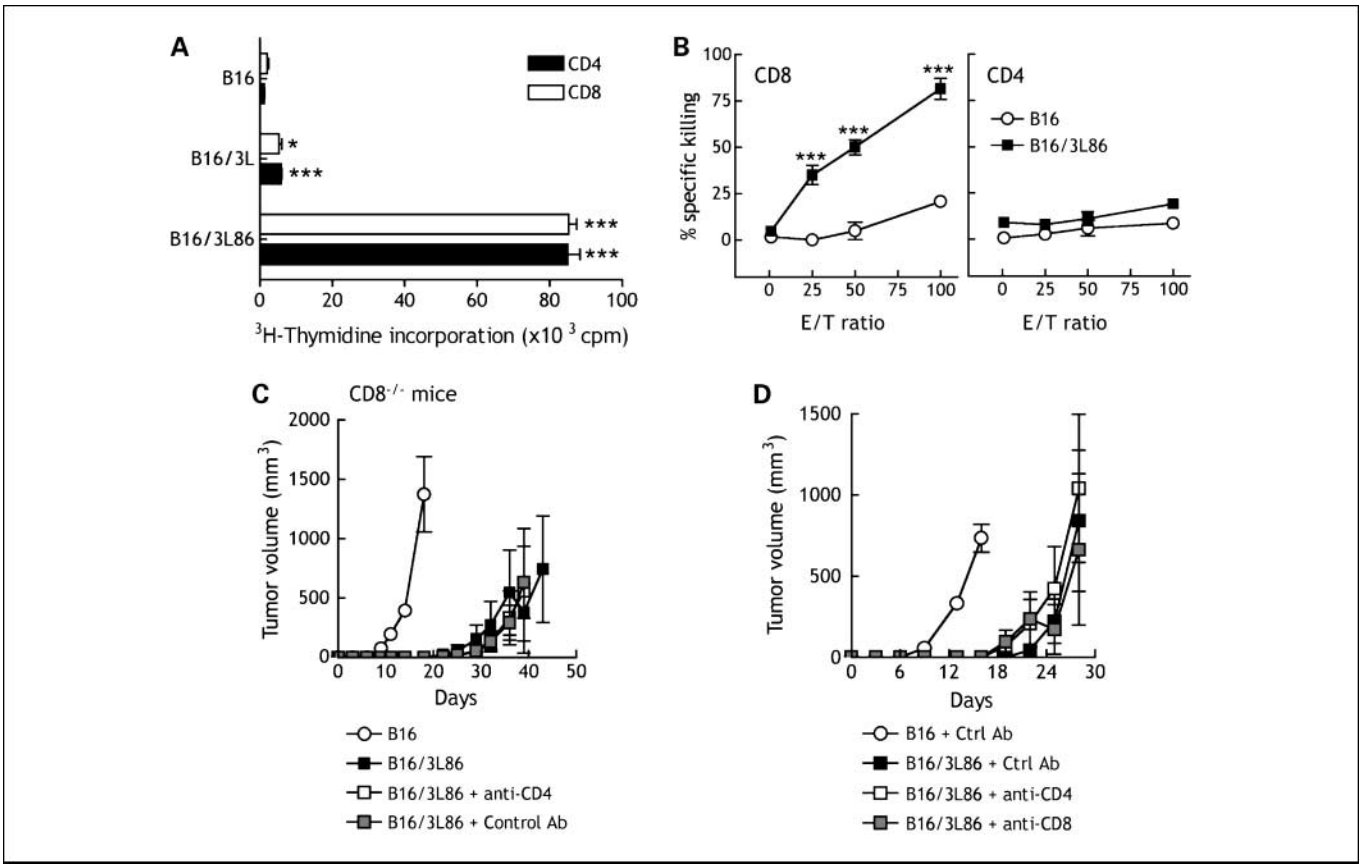

Fig. 3. *In vitro* activation of $CD4^+$ and $CD8^+$ T cells and their role in primary tumor rejection. *A,* naïve $CD4^+$ or $CD8^+$ T cells were incubated in triplicate with the indicated B16 transfectants at a ratio of 10:1 for 48 h before [^{3}H]thymidine incorporation was measured. Bars, SE. *, $P \leq 0.05$; ***, $P \leq 0.0001$, significant differences between T cells stimulated with B16 cells or B16 transfectants. *B,* B16 or B16/3L86 tumor cells prelabeled with [^{3}H]thymidine were coincubated with naïve $CD4^+$ or $CD8^+$ T cells at the indicated T-cell/tumor cell (*E*/*T*) ratios for 72 h. Significance between B16 and B16/3L86 groups at the same T cell/tumor cell ratio is indicated: ***, $P \leq 0.001$. *C,* $CD8^{-/-}$ mice ($n = 7$) were s.c. injected with 2×10^6 B16 cells or B16/3L86 cells on day 0 and tumor growth was monitored. Some mice also received i.p. injections of control antibody or anti-CD4 antibody to deplete $CD4^+$ T cells. *D,* groups of C57BL/6 mice were s.c. injected with 2×10^6 B16 cells or B16/3L86 cells on day 0. Specific T cells were depleted by i.p. injection of anti-CD4 or anti-CD8 antibodies.

mice developed protective immunity against unmodified B16 tumor cells after successful rejection of B16/3L86 tumors (Fig. 2B). These results suggested that antitumor $CD8^+$ T cells were activated by B16/3L86 cells, but their cytolytic activity was suppressed in primary B16/3L86 tumors. Accumulation of $CD4^+CD25^+FoxP3^+$ Tregs in B16 tumors can suppress T-cell–mediated antitumor immunity (29). Low doses of cyclophosphamide, an antineoplastic alkylating agent, can decrease the number and/or function of Tregs (25, 35). To assess whether $CD8^+$ T-cell function could be restored by systemic depletion of Tregs, groups of C57/BL6 mice were i.p. injected with PBS or low-dose cyclophosphamide (2 mg/mouse) 1 day before they were s.c. transplanted with B16 or B16/3L86 cells. This dose of cyclophosphamide has previously been shown to selectively deplete Tregs (23, 35). All mice pretreated with low-dose cyclophosphamide completely rejected B16/3L86 tumors (Fig. 5A). By contrast, cyclophosphamide did not affect the growth of B16 tumors. Periodic administration of low-dose cyclophosphamide enhanced B16/3L86 tumor rejection but was not more effective than a single injection given 1 day before tumor inoculation; four of five mice that received cyclophosphamide treatment on days -1 and 20 remained tumor-free after injection of B16/3L86 tumor cells, and 100% of mice repetitively treated with low-dose cyclophosphamide on days -1, 20, and 40 remained tumor-free (data not shown). Subsequent experiments therefore used a single i.p. injection of 2 mg cyclophosphamide on day -1. To confirm these results, Tregs were depleted by i.p. injection of an anti-CD25 antibody on day -4. The dose and timing we used were previously shown to selectively deplete/inhibit Tregs (24). In agreement with low-dose cyclophosphamide treatment, 100% of mice treated with anti-CD25 antibody remained tumor-free after injection of B16/3L86 cells (Fig. 5B). These results show that depletion of Tregs greatly enhanced rejection of B16 tumor cells expressing CD3L and CD86. To determine the mechanism by which depletion of Tregs enhanced antitumor immunity, $CD8^{-/-}$ mice were treated with low-dose cyclophosphamide before challenge with B16/3L86 cells. In contrast to wt C57BL/6 mice, B16/3L86 tumors eventually progressed in $CD8^{-/-}$ mice after low-dose cyclophosphamide treatment (Supplementary Fig. S4), showing that $CD8^+$ T cells were required for the enhanced antitumor activity observed after depletion of Tregs by low-dose cyclophosphamide treatment. To determine if long-term protective immunity against B16 tumors required T cells, mice that rejected B16/3L86 tumors were depleted of $CD4^+$ or $CD8^+$ T cells before rechallenge with wt B16 tumor cells. Mice treated with control antibody completely rejected B16 tumors, whereas mice depleted of $CD8^+$ T cells developed tumors within 11 days

and mice depleted of $CD4^+$ T cells were only partially protected (Fig. 5C). Thus, the long-term protective immunity generated by B16/3L86 tumors depended on both $CD8^+$ and $CD4^+$ T cells.

Low-dose cyclophosphamide increases activated $CD8^+$ T cells in B16/3L86 tumors. TILs play an important role in the management of tumor growth (36). TILs could not be retrieved from subcutaneous B16/3L86 tumors at early times due to their slow growth. We therefore examined lymphocyte infiltration in B16 peritoneal tumors. Groups of mice were i.p. injected with B16 or B16/3L86 cells and peritoneal lymphocytes were recovered 5 and 8 days later. On day 5, very few lymphocytes could be retrieved from mice injected with B16 cells. On the other hand, abundant lymphocytes were present in B16/3L86 tumors on day 5. On day 8, the numbers of NKT, $CD4^+$, and $CD8^+$ T cells were higher in B16/3L86 cell–injected mice as compared with mice bearing B16 i.p. tumors. By contrast, more NK cells accumulated in the peritoneum of B16 tumor–grafted mice (Supplementary Fig. S5). All TIL populations declined 11 days after i.p. injection of B16 or B16/3L86 tumor cells (data not shown), possibly due to reduced numbers of B16/3L86 cancer cells or suppression of lymphocyte infiltration in advanced B16 tumors. $CD8^+$ effector cells and Tregs isolated from peritoneal tumors on day 8 were also analyzed. Effector $CD8^+$ T cells, which produce IFN-γ, composed 20% to 30% of the $CD8^+$ T-cell population in B16 and B16/3L86 i.p. tumors. Low-dose cyclophosphamide treatment robustly increased the number of IFN-γ^+ $CD8^+$ T cells and decreased the number of Tregs in B16/3L86 tumors (Supplementary Fig. S5). Thus, the ratio of $CD8^+$ IFN-γ^+ T cells to Tregs in peritoneal B16/3L86 tumors increased significantly after treatment with low-dose cyclophosphamide (Fig. 5D).

Tumor-located CD3L and CD86 can create a tumor-destructive environment. The ability of tumor cells expressing CD3L and CD86 to activate NKT cells raised the possibility that unmodified neighboring tumor cells could also be suppressed by intratumorally activated lymphocytes. To test this idea, B16 melanoma cells were mixed with equal numbers of B16/3L86 cells, 3T3 cells, or 3T3/3L86 cells before they were s.c. injected in mice. 3T3/3L86 cells are mouse fibroblasts engineered to stably express CD3L and CD86 on their surface. Mice injected with B16 tumor cells alone or with a mixture of B16 and 3T3 cells developed tumors before day 10. By contrast, tumors grew significantly slower in mice inoculated with a mixture of B16 and B16/3L86 cells or B16 and 3T3/3L86 cells (Fig. 6A). Similarly, s.c. injection of a mixture of 3T3/3L86 cells and TSA breast adenocarcinoma cells resulted in significantly slower tumor growth (Fig. 6B). Thus, CD3L and CD86 can induce a tumor-destructive environment to kill bystander tumor cells. To further investigate the therapeutic potential of membrane-tethered anti-CD3 antibodies for cancer therapy, we constructed adenoviral vectors expressing CD3L (Ad/3L), membrane-tethered anti-phOx control antibody (Ad/Ox), CD86 (Ad/86), or anti-CD28 scFv (Ad/28L). The membrane-tethered anti-CD28 antibody was examined to potentially provide costimulation via CD28 ligation without modulating T-cell activity by ligation of CTLA-4. *In vitro* transfection assays showed that the recombinant adenoviruses expressed the

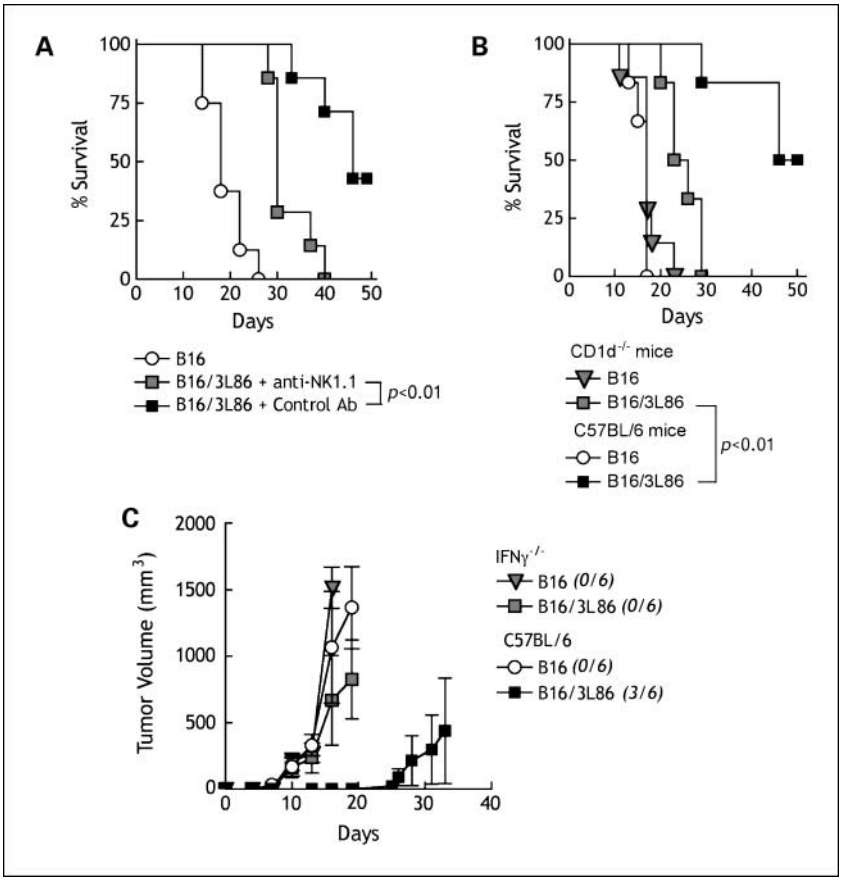

Fig. 4. NKT cells are essential for the antitumor activity induced by CD3L and CD86. *A,* groups of seven C57BL/6 mice were s.c. injected with 2×10^6 B16 or B16/3L86 cells on day 0. Mice were also i.p. injected with anti-NK1.1 or control antibody and mouse survival was followed. *B,* groups of C57BL/6 or $CD1d^{-/-}$ mice ($n = 6$) were s.c. injected with 2×10^6 B16 or B16/3L86 cells on day 0 and mouse survival was monitored. *C,* C57BL/6 or IFN-$\gamma^{-/-}$ mice ($n = 6$) were s.c. transplanted with 1×10^6 B16 or B16/3L86 cells on day 0 and tumor growth was followed. Bars, SE.

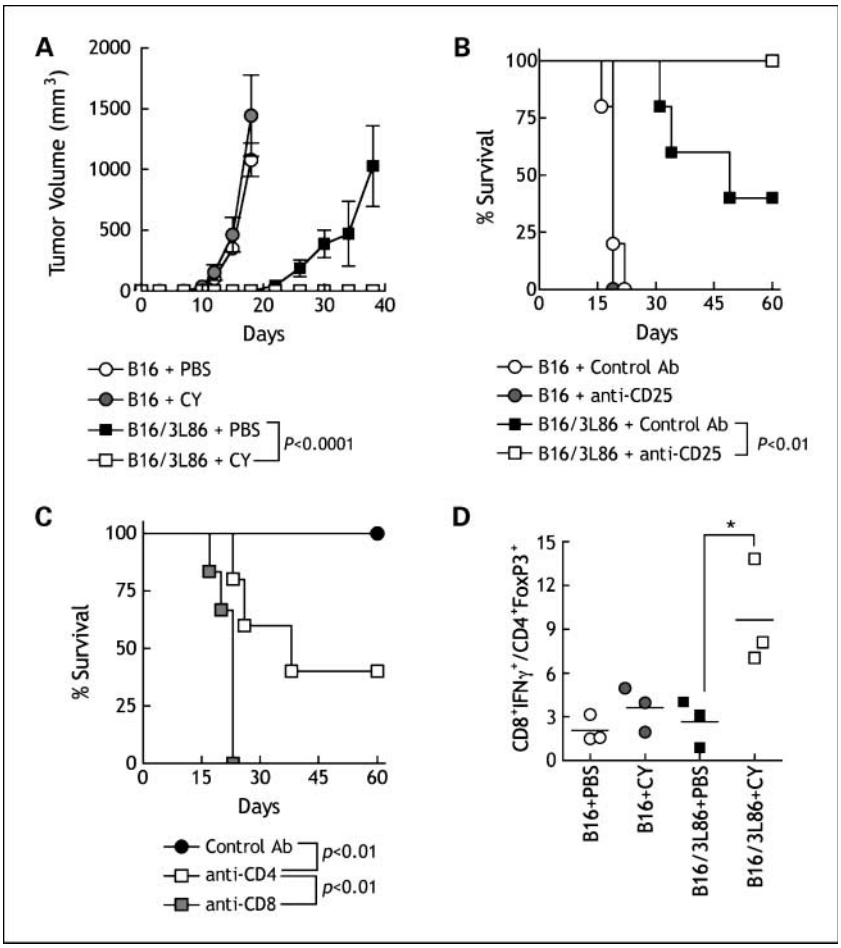

Fig. 5. Treg depletion enhances suppression of B16/3L86 tumors. *A,* C57BL/6 mice ($n = 5$) were i.p. injected with 2 mg cyclophosphamide (*CY*) or PBS on day -1 and then s.c. injected with 2×10^6 B16 or B16/3L86 cells on day 0. Points, mean tumor size; bars, SE. *B,* survival of mice injected with 200 μg of anti-CD25 antibody or control antibody 4 d before s.c. inoculation of 2×10^6 tumor cells. *C,* cyclophosphamide-treated mice that remained tumor-free 60 d after s.c. inoculation of 2×10^6 B16/3L86 cells were i.p. injected with anti-CD4, anti-CD8, or control antibody and then challenged with 10^5 B16 cells. *D,* ratio of peritoneal IFN-γ-producing $CD8^+$ T cells versus Tregs with or without cyclophosphamide treatment. *, $P < 0.05$, significant differences between B16/3L86 groups with and without cyclophosphamide treatment.

appropriate transgenes (Supplementary Fig. S6). Intratumoral injection of B16 tumors with Ad/3L and Ad/86 produced modest delay in the growth of subcutaneous tumors (Supplementary Fig. S7). The modest response of B16 tumors to adenoviral therapy may be related to the poor infectivity of B16 cells by recombinant adenovirus (Supplementary Fig. S8). We therefore tested adenoviral therapy of TSA breast adenocarcinoma tumors because TSA cells were more easily infected by adenovirus vectors (Supplementary Fig. S8). Intratumoral injection of TSA tumors with combinations of either Ad/3L and Ad/86 or Ad/3L and Ad/28L significantly suppressed tumor growth (Fig. 6C). One of eight mice experienced complete tumor regression when treated with Ad/3L and Ad/28L.

Discussion

Tumor-located activation of lymphocytes by membrane-tethered antibodies is under investigation for the therapy of poorly immunogenic tumors (reviewed in ref. 8). In this study, we expressed a membrane-tethered anti-CD3 antibody (CD3L) on poorly immunogenic melanoma cells to activate $CD3^+$ lymphocytes locally in tumors. CD86 was also expressed on the cancer cells to provide costimulation to more completely activate T cells and promote generation of memory $CD8^+$ T cells (37, 38). We expected that local activation of tumor-infiltrating T cells via ligation of CD3 would provide strong antitumor activity without the side effects associated with systemic T-cell activation by CD3 ligation (2). Indeed, expression of CD3L and CD86 on the surface of B16 melanoma cells provided strong antitumor activity and suppressed the growth of subcutaneous, peritoneal, and metastatic tumors. Surprisingly, both $CD4^+$ and $CD8^+$ T cells were totally dispensable for the suppression of primary tumor growth. Rather, we found that tumor suppression was largely mediated by NKT cells. However, chemical or antibody depletion of Treg cells greatly enhanced local T-cell antitumor activity and produced complete rejection of primary tumors. Thus, in combination with Treg depletion, membrane-tethered anti-CD3 scFv along with CD86 effectively activated both innate and adaptive immune responses to control tumor growth.

Our study is the first to show that NKT cells play a critical role in the antitumor activity induced by dual engagement of CD3 and CD28. B16/3L86 tumors progressed more rapidly after depletion of $NK1.1^+$ cells (Fig. 4A) or when transplanted into $CD1d^{-/-}$ mice (Fig. 4B), showing a major role for NKT cells in suppression of tumor cells expressing CD3L and CD86. T cells were dispensable for suppression of primary tumor growth because antibody depletion of $CD4^+$ and $CD8^+$ T cells did not dampen antitumor activity against B16/3L86 tumors (Fig. 3D) and B16/3L86 tumor growth was still significantly delayed in $CD8^{-/-}$ mice, even when $CD4^+$ T cells were also depleted (Fig. 3C). Distinct populations of NKT cells exhibit diverse effects on immunoregulation and tumor suppression (39). Because depletion of $CD4^+$ or $CD8^+$ cells did not affect primary

antitumor activity, the effector NKT cells in our study were likely $CD1d^+CD4^-CD8^-NK1.1^+$. These NKT cells may be similar to liver-derived $CD4^-$ NKT cells that were shown to mediate rejection of MCA and B16F10 tumors in mice (39). NKT cells can initiate both innate and adaptive immune responses, largely by secreting IFN-γ to promote activation of $CD8^+$ T cells and NK cells (40). IFN-γ also directly suppressed the growth of B16 cells and B16 transfectants (Supplementary Fig. S3). Our data showing complete loss of B16/3L86 tumor suppression in IFN-$\gamma^{-/-}$ mice indicate a major role for IFN-γ secretion by NKT cells in the antitumor activity induced by membrane-tethered anti-CD3 antibodies.

$CD4^+CD25^+FoxP3^+$ Tregs accumulate in the spleen, tumors, and draining lymph nodes of mice bearing B16 tumors (29). Systemic depletion of Tregs with anti-CD25 or low-dose cyclophosphamide treatment can promote rejection of tumors in mice (24–26). In our study, depletion of Tregs with either anti-CD25 antibodies or low-dose cyclophosphamide dramatically increased the life span of mice injected with B16/3L86 tumors with up to 100% long-term survivors. Besides $CD4^+$ and $CD8^+$ T cells, Tregs have also been reported to suppress the function of NKT cells (17, 41). However, the beneficial effects of Treg depletion by low-dose cyclophosphamide were completely lost in $CD8^{-/-}$ mice (Supplementary Fig. S4), indicating that Tregs mainly suppressed local $CD8^+$ T-cell function rather than NKT cell antitumor activity. Likewise, cyclophosphamide treatment significantly increased the ratio of activated IFN-γ^+CD8^+ T cells to $CD4^+FoxP3^+$ T cells in B16/3L86 tumors (Fig. 5D), indicating that the activity of tumor-infiltrating $CD8^+$ T cells was restored on depletion of Tregs. Interestingly, effective antitumor memory was induced against B16 melanoma cells regardless of whether Tregs were depleted (Figs. 2B and 5C). Taken together, these results indicate that $CD8^+$ T cells and NKT cells were effectively activated in B16/3L86 tumors

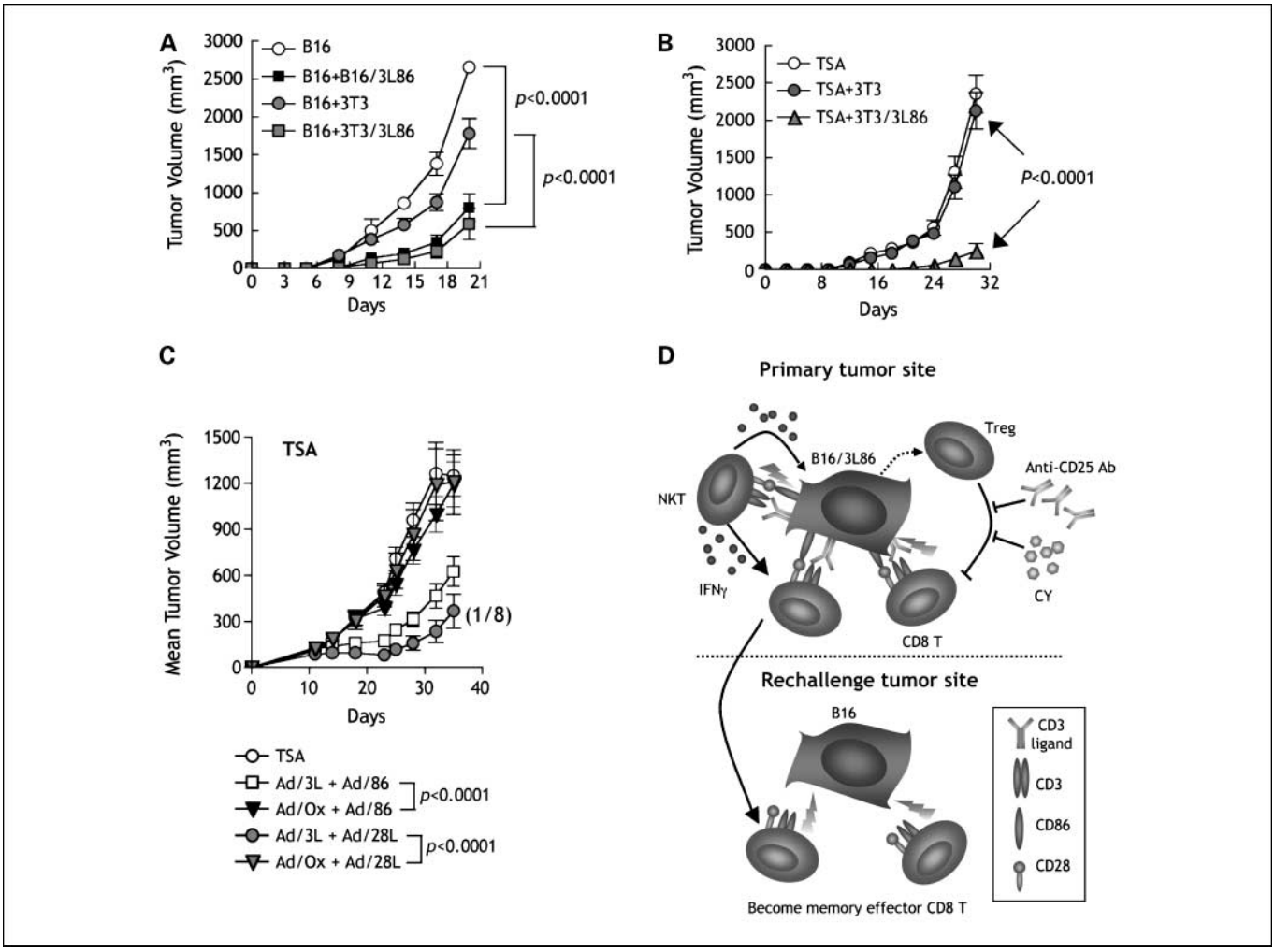

Fig. 6. Cells expressing CD3L and CD86 induce a tumor-destructive environment. *A,* groups of five C57BL/6 mice were s.c. injected with 2×10^6 B16 cells in combination with or without 2×10^6 B16/3L86, 3T3, or 3T3/3L86 cells on day 0, and tumor size was monitored. *B,* groups of five BALB/c mice were s.c. inoculated with 5×10^5 TSA tumor cells in mixture with or without 2×10^6 3T3 or 3T3/3L86 cells on day 0. *C,* BALB/c mice ($n = 8$) were s.c. injected with 5×10^5 TSA tumor cells on day 0. Mice received intratumoral injections of the indicated adenoviruses on days 11 and 12. *D,* hypothetical model of membrane-anchored CD3 ligand and CD86-induced antitumor activity. Tumor-infiltrating T cells and NKT cells are activated by ligation of CD3 and CD28. NKT cells are responsible for initial tumor suppression because Tregs suppress local $CD8^+$ T-cell activity but not $CD8^+$ T-cell differentiation into memory T cells. IFN-γ secreted by NKT cells may suppress tumor growth and promote long-term T memory response. Memory $CD8^+$ T cells can mediate rejection of wt B16 tumors. Systemic reduction of Tregs with low-dose cyclophosphamide or anti-CD25 antibody enhances $CD8^+$ T-cell antitumor activity in tumors.

(Fig. 6D). Tregs seemed to suppress local $CD8^+$ T-cell antitumor activity but not their differentiation into memory T cells. Hence, mice were protected from rechallenge with parental B16 melanoma cells, suggesting that activated memory $CD8^+$ T cells could recognize low levels of tumor-associated antigens presented by MHC molecules on B16 cancer cells. In addition, Tregs did not seem to suppress NKT cells, which accounted for most of the antitumor activity against B16/3L86 tumors. Systemic depletion of Tregs unmasked local $CD8^+$ T-cell antitumor activity, which, in concert with NKT cells, entirely eradicated B16/3L86 tumors.

Besides NKT cells and $CD8^+$ T cells, CD3L and CD86 also effectively activated $CD4^+$ T cells (Fig. 3A), and B16/3L86 cells induced the expansion of $CD4^+$ T cells inside peritoneal tumors (Supplementary Fig. S5). $CD4^+$ T cells are critical for generation of $CD8^+$ T-cell–dependent memory responses (42). The strong memory response observed against parental B16 melanoma cells in mice that rejected B16/3L86 tumors suggests that coactivation of both $CD4^+$ and $CD8^+$ T cells may promote effective T-cell memory responses. Indeed, whereas depletion of $CD8^+$ T cells completed abrogated antitumor memory responses, depletion of $CD4^+$ T cells also hindered antitumor memory (Fig. 5C). The development of long-term antitumor immunity implies that T cells with specificity for tumor antigens infiltrated B16/3L86 tumors and were activated by CD3 and CD28 ligation. This is consistent with previous studies showing that lymphocytes recovered from human melanomas display specificity for melanoma-associated antigens (43, 44). Our results indicate that CD3L and CD86 produce sufficient *in vivo* activation and expansion of melanoma-specific T cells to effectively generate antitumor memory.

Our study revealed that CD3L and CD86 suppressed the growth of tumor cells expressing these molecules and also helped control the growth of neighboring cancer cells. This is important because cancer cells can escape immunosurveillance by down-regulating expression of MHC molecules or tumor antigens, eventually leading to tumor repopulation and treatment failure (45). Expression of tumor antigens at low levels can also result in partial activation of TILs and poor antitumor activity (46). Fibroblasts engineered to express CD3L and CD86 induced *in vivo* bystander killing of neighboring B16 melanoma or TSA breast carcinoma cells, which may help overcome antigen escape mutants. Expression of membrane-tethered anti-CD3 scFv with CD86 may help harness the immune system for the therapy of otherwise poorly immunogenic tumors.

Preliminary studies in which solid tumors were directly injected with recombinant adenoviruses expressing CD3L and CD86 or membrane-tethered anti-CD28 scFv showed good antitumor activity. We did not observe obvious side effects, suggesting that this approach may be clinically useful. A future challenge is to use delivery vectors such as recombinant viruses, cell delivery systems, or bispecific antibodies to locally ligate CD3 and CD28 on lymphocytes present in tumors.

Expression of membrane-tethered anti-CD3 scFv on tumors mimics anti-CD3–based bispecific antibodies, which are novel reagents designed to bind both tumor-associated surface antigens and CD3 on T cells. Bispecific antibodies, as well as newer, highly potent reagents such as bispecific T-cell engager molecules, are under clinical development for the treatment of cancer (3–5, 7, 47). Our results showing that $CD3^+$ NKT cells can be activated by membrane-tethered CD3 scFv to provide potent antitumor activity implies that NKT cells may also be important for the antitumor activity of bispecific antibodies. Stimulation of NKT cells, for example by systemic administration of stimulatory glycolipids, may be a rational approach to enhance the efficacy of CD3L therapy as well as anti-CD3 bispecific antibody therapy (48, 49). Our results also suggest that, in common with membrane-tethered anti-CD3, bispecific antibody therapy may also be improved by depleting Tregs.

In summary, we investigated the mechanism of tumor-located lymphocyte activation by membrane-tethered anti-CD3 antibody and CD86. We found that NKT cells play an important role in mediating primary tumor rejection in the presence of Tregs, whereas both NKT cells and $CD8^+$ T cells provided strong antitumor activity after Tregs were depleted from mice. Importantly, memory antitumor T cells were effectively generated even in the presence of Tregs. Furthermore, expression of anti-CD3 scFv and CD86 on cells induced bystander cytotoxicity to neighboring cancer cells in tumors. Local expression of membrane-tethered CD3 scFv and CD86 created a tumor destruction environment that may lead to clinical approaches for cancer therapy.

Disclosure of Potential Conflicts of Interest

No potential conflicts of interest were disclosed.

Acknowledgments

We thank Dr. C. Wang for generously providing CD1d-deficient ($CD1d^{-/-}$) mice and Dr. Sebastian Tuve from the University of Washington in Seattle for helpful suggestions.

References

1. Sosman JA, Weiss GR, Margolin KA, et al. Phase IB clinical trial of anti-CD3 followed by high-dose bolus interleukin-2 in patients with metastatic melanoma and advanced renal cell carcinoma: clinical and immunologic effects. J Clin Oncol 1993;11:1496–505.
2. Chatenoud L, Ferran C, Bach JF. The anti-CD3-induced syndrome: a consequence of massive *in vivo* cell activation. Curr Top Microbiol Immunol 1991;174:121–34.
3. Reusch U, Sundaram M, Davol PA, et al. Anti-CD3 x anti-epidermal growth factor receptor (EGFR) bispecific antibody redirects T-cell cytolytic activity to EGFR-positive cancers *in vitro* and in an animal model. Clin Cancer Res 2006;12:183–90.
4. Kiewe P, Hasmuller S, Kahlert S, et al. Phase I trial of the trifunctional anti-HER2 x anti-CD3 antibody ertumaxomab in metastatic breast cancer. Clin Cancer Res 2006;12:3085–91.
5. Burges A, Wimberger P, Kumper C, et al. Effective relief of malignant ascites in patients with advanced ovarian cancer by a trifunctional anti-EpCAM x anti-CD3 antibody: a phase I/II study. Clin Cancer Res 2007;13:3899–905.
6. Muller D, Kontermann RE. Recombinant bispecific antibodies for cellular cancer immunotherapy. Curr Opin Mol Ther 2007;9:319–26.
7. Bargou R, Leo E, Zugmaier G, et al. Tumor regression in cancer patients by very low doses of a T-cell–engaging antibody. Science 2008;321:974–7.
8. Cheng TL, Roffler S. Membrane-tethered proteins for basic research, imaging, and therapy. Med Res Rev 2008;28:885–928.
9. Liao KW, Chen BM, Liu TB, et al. Stable expression of chimeric anti-CD3 receptors on mammalian cells for stimulation of antitumor immunity. Cancer Gene Ther 2003;10:779–90.
10. Liao KW, Lo YC, Roffler SR. Activation of lymphocytes by anti-CD3 single-chain antibody dimers expressed on the plasma membrane of tumor cells. Gene Ther 2000;7:339–47.
11. Paul S, Regulier E, Rooke R, et al. Tumor gene therapy by MVA-mediated expression of T-cell-stimulating antibodies. Cancer Gene Ther 2002;9:470–7.

12. Paul S, Regulier E, Poitevin Y, Hormann H, Acres RB. The combination of a chemokine, cytokine and TCR-based T cell stimulus for effective gene therapy of cancer. Cancer Immunol Immunother 2002;51: 645–54.

13. Ye Z, Hellstrom I, Hayden-Ledbetter M, Dahlin A, Ledbetter JA, Hellstrom KE. Gene therapy for cancer using single-chain Fv fragments specific for 4-1BB. Nat Med 2002;8:343–8.

14. Yang Y, Yang S, Ye Z, et al. Tumor cells expressing anti-CD137 scFv induce a tumor-destructive environment. Cancer Res 2007;67:2339–44.

15. Gruel N, Fridman WH, Teillaud JL. Bypassing tumor-specific and bispecific antibodies: triggering of antitumor immunity by expression of anti-FcγR scFv on cancer cell surface. Gene Ther 2001;8:1721–8.

16. Zou W. Regulatory T cells, tumour immunity and immunotherapy. Nat Rev Immunol 2006;6:295–307.

17. Nishikawa H, Kato T, Tanida K, et al. $CD4^+$ $CD25^+$ T cells responding to serologically defined autoantigens suppress antitumor immune responses. Proc Natl Acad Sci U S A 2003;100:10902–6.

18. Khong HT, Restifo NP. Natural selection of tumor variants in the generation of "tumor escape" phenotypes. Nat Immunol 2002;3:999–1005.

19. Curiel TJ, Coukos G, Zou L, et al. Specific recruitment of regulatory T cells in ovarian carcinoma fosters immune privilege and predicts reduced survival. Nat Med 2004;10:942–9.

20. Woo EY, Yeh H, Chu CS, et al. Cutting edge: regulatory T cells from lung cancer patients directly inhibit autologous T cell proliferation. J Immunol 2002;168: 4272–6.

21. Viguier M, Lemaitre F, Verola O, et al. Foxp3 expressing $CD4^+CD25$(high) regulatory T cells are overrepresented in human metastatic melanoma lymph nodes and inhibit the function of infiltrating T cells. J Immunol 2004;173:1444–53.

22. Liyanage UK, Moore TT, Joo HG, et al. Prevalence of regulatory T cells is increased in peripheral blood and tumor microenvironment of patients with pancreas or breast adenocarcinoma. J Immunol 2002;169: 2756–61.

23. Tuve S, Chen BM, Liu Y, et al. Combination of tumor site-located CTL-associated antigen-4 blockade and systemic regulatory T-cell depletion induces tumor-destructive immune responses. Cancer Res 2007;67: 5929–39.

24. Shimizu J, Yamazaki S, Sakaguchi S. Induction of tumor immunity by removing $CD25^+CD4^+$ T cells: a common basis between tumor immunity and autoimmunity. J Immunol 1999;163:5211–8.

25. Ghiringhelli F, Larmonier N, Schmitt E, et al. $CD4^+$ $CD25^+$ regulatory T cells suppress tumor immunity but are sensitive to cyclophosphamide which allows immunotherapy of established tumors to be curative. Eur J Immunol 2004;34:336–44.

26. Ercolini AM, Ladle BH, Manning EA, et al. Recruitment of latent pools of high-avidity CD8(+) T cells to the antitumor immune response. J Exp Med 2005; 201:1591–602.

27. Lanier LL. NK cell recognition. Annu Rev Immunol 2005;23:225–74.

28. Kronenberg M. Toward an understanding of NKT cell biology: progress and paradoxes. Annu Rev Immunol 2005;23:877–900.

29. Sutmuller RP, van Duivenvoorde LM, van Elsas A, et al. Synergism of cytotoxic T lymphocyte-associated antigen 4 blockade and depletion of CD25(+) regulatory T cells in antitumor therapy reveals alternative pathways for suppression of autoreactive cytotoxic T lymphocyte responses. J Exp Med 2001;194: 823–32.

30. Kaartinen M, Griffiths GM, Hamlyn PH, et al. Anti-oxazolone hybridomas and the structure of the oxazolone idiotype. J Immunol 1983;130:937–45.

31. Kim HJ, Kim HY, Kim BK, Kim S, Chung DH. Engagement of glucocorticoid-induced TNF receptor costimulates NKT cell activation *in vitro* and *in vivo*. J Immunol 2006;176:3507–15.

32. Hashimoto W, Tanaka F, Robbins PD, et al. Natural killer, but not natural killer T, cells play a necessary role in the promotion of an innate antitumor response induced by IL-18. Int J Cancer 2003;103:508–13.

33. Smyth MJ, Crowe NY, Pellicci DG, et al. Sequential production of interferon-γ by NK1.1(+) T cells and natural killer cells is essential for the antimetastatic effect of α-galactosylceramide. Blood 2002;99:1259–66.

34. Talmadge JE, Tribble HR, Pennington RW, Phillips H, Wiltrout RH. Immunomodulatory and Immunotherapeutic Properties of Recombinant γ-Interferon and Recombinant Tumor Necrosis Factor in Mice. Cancer Res 1987;47:2563–70.

35. Lutsiak ME, Semnani RT, De Pascalis R, Kashmiri SV, Schlom J, Sabzevari H. Inhibition of CD4(+)25+ T regulatory cell function implicated in enhanced immune response by low-dose cyclophosphamide. Blood 2005;105:2862–8.

36. Yu P, Fu YX. Tumor-infiltrating T lymphocytes: friends or foes? Lab Invest 2006;86:231–45.

37. Alegre ML, Frauwirth KA, Thompson CB. T-cell regulation by CD28 and CTLA-4. Nat Rev Immunol 2001; 1:220–8.

38. Borowski AB, Boesteanu AC, Mueller YM, et al. Memory $CD8^+$ T cells require CD28 costimulation. J Immunol 2007;179:6494–503.

39. Crowe NY, Coquet JM, Berzins SP, et al. Differential antitumor immunity mediated by NKT cell subsets *in vivo*. J Exp Med 2005;202:1279–88.

40. Liu K, Idoyaga J, Charalambous A, et al. Innate NKT lymphocytes confer superior adaptive immunity via tumor-capturing dendritic cells. J Exp Med 2005; 202:1507–16.

41. Azuma T, Takahashi T, Kunisato A, Kitamura T, Hirai H. Human $CD4^+$ $CD25^+$ regulatory T cells suppress NKT cell functions. Cancer Res 2003;63:4516–20.

42. Klebanoff CA, Gattinoni L, Restifo NP. $CD8^+$ T-cell memory in tumor immunology and immunotherapy. Immunol Rev 2006;211:214–24.

43. Benlalam H, Labarriere N, Linard B, et al. Comprehensive analysis of the frequency of recognition of melanoma-associated antigen (MAA) by CD8 melanoma infiltrating lymphocytes (TIL): implications for immunotherapy. Eur J Immunol 2001;31: 2007–15.

44. Kawakami Y, Eliyahu S, Sakaguchi K, et al. Identification of the immunodominant peptides of the MART-1 human melanoma antigen recognized by the majority of HLA-A2-restricted tumor infiltrating lymphocytes. J Exp Med 1994;180:347–52.

45. Zitvogel L, Tesniere A, Kroemer G. Cancer despite immunosurveillance: immunoselection and immunosubversion. Nat Rev Immunol 2006;6:715–27.

46. Gervois N, Guilloux Y, Diez E, Jotereau F. Suboptimal activation of melanoma infiltrating lymphocytes (TIL) due to low avidity of TCR/MHC-tumor peptide interactions. J Exp Med 1996;183:2403–7.

47. Hammond SA, Lutterbuese R, Roff S, et al. Selective targeting and potent control of tumor growth using an EphA2/CD3-Bispecific single-chain antibody construct. Cancer Res 2007;67:3927–35.

48. Chang DH, Osman K, Connolly J, et al. Sustained expansion of NKT cells and antigen-specific T cells after injection of α-galactosyl-ceramide loaded mature dendritic cells in cancer patients. J Exp Med 2005; 201:1503–17.

49. Chang Y-J, Huang J-R, Tsai Y-C, et al. Potent immune-modulating and anticancer effects of NKT cell stimulatory glycolipids. Proc Natl Acad Sci U S A 2007;104:10299–304.